THE JOURNAL OF BIOLOGICAL CHEMISTRY VOL. 286, NO. 31, pp. 27676–27686, August 5, 2011

Growth Arrest Specific 8 (Gas8) and G Protein-coupled Receptor Kinase 2 (GRK2) Cooperate in the Control of Smoothened Signaling*[S]

Received for publication, February 24, 2011, and in revised form, May 25, 2011 Published, JBC Papers in Press, June 8, 2011, DOI 10.1074/jbc.M111.234666

Tama Evron[‡1], **Melanie Philipp**[‡2,3], **Jiuyi Lu**[§], **Alison R. Meloni**[‡], **Martin Burkhalter**[¶], **Wei Chen**[§], **and Marc G. Caron**[‡4]

From the Departments of [‡]*Cell Biology and* [§]*Medicine, Duke University Medical Center, Durham, North Carolina 27710 and* [¶]*Department of Molecular Medicine and Max Planck Research Group on Stem Cell Aging, Albert Einstein Allee 11, University of Ulm, Ulm 89081, Germany*

The G protein-coupled receptor (GPCR)-like molecule Smoothened (Smo) undergoes dynamic intracellular trafficking modulated by the microtubule associated kinase GRK2 and recruitment of β-arrestin. Of this trafficking, especially the translocation of Smo into primary cilia and back to the cytoplasm is essential for the activation of Hedgehog (Hh) signaling in vertebrates. The complete mechanism of this bidirectional transport, however, is not completely understood. Here we demonstrate that Growth Arrest Specific 8 (Gas8), a microtubule associated subunit of the Dynein Regulatory Complex (DRC), interacts with Smo to modulate this process. Gas8 knockdown in ciliated cells reduces Smo signaling activity and ciliary localization whereas overexpression stimulates Smo activity in a GRK2-dependent manner. The C terminus of Gas8 is important for both Gas8 interaction with Smo and facilitating Smo signaling. In zebrafish, knocking down Gas8 results in attenuated Hh transcriptional responses and impaired early muscle development. These effects can be reversed by the co-injection of Gas8 mRNA or by constitutive activation of the downstream Gli transcription factors. Furthermore, Gas8 and GRK2 display a synergistic effect on zebrafish early muscle development and some effects of GRK2 knockdown can be rescued by Gas8 mRNA. Interestingly, Gas8 does not interfere with cilia assembly, as the primary cilia architecture is unchanged upon Gas8 knock down or heterologous expression. This is in contrast to cells stably expressing both GRK2 and Smo, in which cilia are significantly elongated. These results identify Gas8 as a positive regulator of Hh signaling that cooperates with GRK2 to control Smo signaling.

Smoothened (Smo)[5] is a G protein-coupled receptor (GPCR)-like protein that serves as the main transducer of the Hedgehog (Hh) signaling pathway, regulating many aspects of embryonic development. Loss of function of components of this pathway leads to human developmental disorders, including holoprosencephaly, polydactyly, craniofacial, and skeletal malformation (1, 2), while inappropriate activation of the pathway is linked to a wide range of malignancies (3). Data from mammalian cell culture, mice, and zebrafish have implicated Smo trafficking into the primary cilia by intraflagellar transport (IFT) particles as an essential step in Hh downstream signaling (reviewed in Refs. 4, 5). Smo translocation results in the accumulation of transcriptionally active Gli (GliA) at the tip of the cilia, which is then transported out of the cilia to promote Hh target gene expression (4). Similar to classic GPCRs, phosphorylation of active Smo by the GPCR kinase 2 (GRK2) and recruitment of β-arrestin results in Smo internalization (6), and both GRK2 and β-arrestin play a positive role in Smo signaling as they do in selective forms of GPCR signaling (7, 8). Interestingly, GRK2 has been reported as a microtubule associated kinase that directly phosphorylates tubulin following GPCR stimulation (9). GRK2 has also been shown to promote signaling through phosphorylation of Smo (10) and enhancement of the direct interaction between Smo and β-arrestin (11). β-Arrestin 2 and GRK2/3 knockdown in zebrafish embryos provides further evidence for their association with the activation of Hh pathway in vertebrates (10, 12). Moreover, β-arrestin was shown to promote Smo translocation into the cilia by mediating its interaction with the kinesin motor protein Kif3A in mammalian cell culture (13).

Growth arrest specific 8 (Gas8, also called Gas11) is the vertebrate homolog of the *Trypanosoma brucei* protein trypanin (14, 15) and *Chlamydomonas* paralyzed flagellar 2 (PF2), in which mutations lead to defective flagella motility (16). This conserved family of microtubule-associated proteins encodes for the Dynein Regulatory Complex (DRC) subunit 4 (15, 16). Several different domains within Gas8 have been identified with different affinities for microtubules, including a microtu-

* This work was supported, in whole or in part, by National Institutes of Health Grants NS19576 and MH073853.

[S] The on-line version of this article (available at http://www.jbc.org) contains supplemental Figs. S1–S3.

[1] Recipient of a postdoctoral fellowship from The Machiah Foundation, a supporting foundation of the Jewish Community Federation of San Francisco, the Peninsula, Marin, & Sonoma Counties.

[2] Present address: Dept. of Biochemistry and Molecular Biology, Albert Einstein Allee 11, University of Ulm, Ulm 89081, Germany.

[3] Recipient of a Marie Curie Outgoing International Fellowship of the European Commission.

[4] To whom correspondence should be addressed: Department of Cell Biology. Box 3287 or RM 487 Carl Bldg., Duke University Medical Center, Durham, NC 27710. Tel.: 919-684-5433; Fax: 919-681-8641; E-mail: caron002@mc.duke.edu.

[5] The abbreviations used are: Smo, smoothened; Hh, hedgehog; Gas8, growth arrest specific 8; GRK2, G protein-coupled receptor kinase 2; DRC, dynein regulatory complex; IFT, intraflagellar transport; GMAD, Gas8 microtubule association domain; IMAD, inhibitor of microtubule association domain; Pol, polaris; shRNA, short hairpin RNA; MO, morpholino; hpf, hours post fertilization.

bule association domain (GMAD) between residues 115–258 and the N-terminal inhibitor of microtubule association domain (IMAD) between residues 1–108 (17). In this study, an engineered protein consisting of the GMAD and C terminus domains of Gas8 ($Gas8_{GMAD\text{-}CT}$) displayed the highest affinity to microtubules. In zebrafish embryos, Gas8 knock down results in abnormal ear development and defective cilia motility (14), providing the first evidence of Gas8 and DRC requirement for proper motile cilia functioning in vertebrates.

Here we show that Gas8 interacts with Smo and functions as a positive regulator of Hh signaling, a pathway dependent on non-motile cilia. In cells we find that Gas8 association with microtubules at the base of cilia and the presence of active GRK2 contribute to the positive effect of Gas8 on Smo signaling. In zebrafish embryos we show that Gas8 is important for proper slow muscle development and Hh-target gene expression, but not for cilia assembly. Altogether, these data are consistent with Gas8 and GRK2 influencing Hh pathway upstream of Gli.

EXPERIMENTAL PROCEDURES

Plasmids—The 16.2 Gli reporter plasmid and the Myc-Smo expression plasmid were obtained from M. Scott, Stanford University (18). The bovine GRK2, and bovine GRK2-K220R expression plasmids were described previously (19). A full-length mouse (m)Gas8 cDNA sequence (NM_018855.2) was cloned into pCDNA6 via NotI and XhoI following an upstream Flag sequence. Flag-Gas8 mutants were cloned in the same way using primer pairs for the indicated amino acids positions (Fig. 2*A*). Full-length and mutant GFP-mGas8 constructs were cloned into the pEGFPC1 plasmid between the BglII and EcoRI sites.

Yeast 2-Hybrid Assay—To identify novel interaction partners of Smo, the C terminus of Smo was cloned in-frame with the Gal4 binding domain into pAS2.1. This bait vector was used to screen a human brain library (Clontech, Palo Alto, CA). For verification of obtained interactions, competent cells of the yeast strain AH109 were co-transformed with the Smo C terminus bait vector and fragments of human Gas8 in frame with the Gal4 activating domain of pACT2 using the Yeastmaker™ Yeast Transformation System 2 (Clontech). As control, empty prey and bait vectors were used to assess growth in the absence of inserts.

RNA Interference—Scramble lentiviral shRNA and mouse Gas8 lentiviral shRNA (SHCLN**G**-NM_018855-TRCN0000195976) were purchased from Sigma. Lentivirus production and shRNA knock-down were performed according to the manufacturer's protocol. Briefly, the shRNA plasmid together with psPAX2 viral packaging plasmid and pMD2.G envelope plasmid (Addgene, Cambridge, MA) were transfected into HEK293T cells. The culture media were harvested 48 h after transfection, spun at 1250 rpm for 5 min at 4 °C, and stored at −80 °C. To generate stable lines, NIH-3T3 cells (ATCC, Manassas, VA) were infected with the lentiviral particles. The medium was changed 1 day postinfection. Positive clones were selected by 1 μg/ml puromycin. We have also tested a second shRNA against Gas8 (SHCLN**G**-NM_018855-TRCN0000179097) that yielded 80% reduction in Gas8 protein and ~70% reduction in the reporter activity, but was eventually deleterious to survival of the cell. Thus, this shRNA was not used further. GFP-Smo cells (13) were infected with the shRNAs to generate double stable lines as above.

Transfections and Luciferase Assay—Luciferase reporter assay in NIH-3T3 cells was performed as described (13). Briefly, NIH-3T3 cells were transfected with 1.05 μg 9× Gli-binding site-luciferase plasmid and 0.15 μg of pRL-TK (Promega, Madison, WI) using Fugene 6 (Roche Diagnostics, Mannheim, Germany) according to the manufacturer's recommendations. Cells were treated with either DMSO or 0.25 μM SAG in DMSO at a final concentration of 0.005% and then lysed in reporter lysis buffer (Promega). Reporter activity was determined by using the Dual-Luciferase Reporter Assay System (Promega). The ctivity of the Firefly luciferase reporter was normalized to the activity of a *Renilla* luciferase internal control for transfection efficiency. Luciferase reporter assay in C3H10T1/2 cells was performed as described (11). Briefly, C3H10T1/2 cells (ATCC) were transfected using TransIT-LT1 reagent (Mirus, Madison, WI) at a density of 2.5×10^5 cells/well in 6-well plate with 0.75 μg of the indicated plasmids along with 0.5 μg of Gli-luciferase reporter and 0.25 μg of CMV-β-galactosidase (β-gal) as transfection control. 3 μg of total DNA amount was complemented with the empty pCDNA3 plasmid. The activity of the luciferase reporter, measured 72 h after transfection, was normalized to the activity of β-gal, For experiments with the antagonist, C3H10T1/2 stable cell lines generated from a pool of transfected cells (11) were treated with 10 μM cyclopamine in DMSO at a final concentration of 0.02% or with DMSO alone for 24 h prior to lysis.

Coimmunoprecipitation Assay—HEK 293 cells plated in 10-cm dish were transiently transfected with 3 μg of Myc-Smo, 2 μg of Flag-Gas8 or both constructs by the calcium phosphate method. DNA amount transfected was kept constant with the empty pcDNA3 plasmid. 48 h post-transfection, cells were harvested in 0.7 ml immunoprecipitation buffer containing 50 mM HEPES, 0.5% Triton X-100, 250 mM NaCl, 10% glycerol, 2 mM EDTA, and a 1× protease inhibitor mixture tablet (Complete; Roche Diagnostics). To avoid interference with the protein-protein interaction, the immunoprecipitation buffer contained non-ionic detergent that mainly solubilizes the cytoplasmic detergent-soluble fraction of Gas8 (20). This fraction may be enriched by the transient transfection of Flag-Gas8 and probably by microtubule de-polymerization in the absence of microtubule-stabilizer (17). An aliquot of the extract (2%) was used as the input, while the remaining extract was incubated with Flag antibody beads (Sigma) that had been pre-blocked with 0.5% bovine serum albumin for 1 h. Extracts and beads were allowed to mix at 4 °C overnight. Beads were then washed four times in the lysis buffer and four times with a high salt lysis buffer (750 mM NaCl). Sample loading buffer was then added directly to the washed beads and run on 10% Tris-glycine polyacrylamide gels (Invitrogen). The gels were transferred to a nitrocellulose membrane, which was then blotted with rabbit anti-Myc (1:2000, abcam, Cambridge, MA) and mouse anti-Flag M2 (1:1500, Sigma).

Immunoblots and Immunofluorescence—Immunoblots were performed according to standard protocols. A rabbit polyclonal

Gas8/11 (Pep5) antibody corresponding to GMAD amino acids 111–127 (NNLTEMKAGTVVMK) was a kind gift from R. H. Crosbie and K. Hill at UCLA, CA. Gas8/11 antibody was diluted 1:500 and yielded a 56 kDa band. Rabbit anti-GFP (FL, 1:1500, Santa Cruz Biotechnology, Santa Cruz, CA) was used to detect Smo in the GFP-Smo cell line and mouse anti-Actin (1:5000, Milipore/Chemicon, Billerica, MA) was used as loading control. The signal was detected by a SuperSignal West Femto maximum-sensitivity substrate (Pierce). For immunofluorecence, C3H10T1/2 cells were transfected using TransIT-LT1 reagent (Mirus, Madison, WI) at a density of 2.5×10^5 cells/35 mm glass bottom culture dish (MatTek, Ashland, MA) with the indicated plasmids, incubated for 48 h and fixed with 4% paraformaldehyde. Samples were incubated in 0.1% Triton for 10 min and blocked in 10% normal goat serum (NGS) for 30 min and then incubated with the primary antibody for either 3 h at room temperature or at 4 °C overnight. Samples were washed in PBS and incubated with the appropriate secondary antibody for 2 h at room temperature. GFP-Smo cells were grown to confluence in 35 mm glass bottom culture dishes, starved for 2 h in 2% BCS, fixed, and stained according to the above protocol. All antibodies were diluted in 1% BSA, 2% NGS, 0.4% Triton X-100 and 0.05% Tween-20 in PBS. Primary antibodies used were: mouse anti-acetylated tubulin (1:1000, Sigma), mouse anti-γ-tubulin (1:500, Sigma), mouse anti-β-tubulin (1:1000, Sigma), rabbit anti-Myc (1:4000, Abcam), rabbit anti-GRK2 C-15 (1:500, Santa Cruz Biotechnology), and rabbit anti-GM130 (1:500, Sigma). Secondary antibodies included Alexa Fluor 568 goat anti-mouse, 568 goat anti-rabbit, and 488 goat anti-rabbit (Invitrogen/Molecular Probes, Eugene, OR). LysoTracker was used to label lysosomes (Invitrogen). DNA was labeled using either Hoechst stain (Invitrogen) or Draq5 (Alexis Biochemicals, San Diego, CA). Imaging was done using Zeiss LSM510 and LSM710 confocal microscopy systems. The public domain ImageJ software was used for the analysis of confocal Z-stacks.

Zebrafish Strains and Husbandry—A single outcross of ekwill and AB inbred lines (EK/AB) produced adult fish that were used for wild-type egg production. *Smo*$^{s294+/-}$ mutants (21) were kindly provided by M. Bagnat, Duke University, intercrossed, and screened for mutant embryos. All zebrafish were maintained according to standard procedures in accordance with Duke University approved animal use IACUC protocols.

Morpholino and mRNA Microinjections—The zGas8 ATG MO (5′-GCGACGATTTTCTTTTTGGTGGCAT-3′) targeting the translation start site of the z*Gas8* mRNA was previously described (14). 5-bp mismatched ATG morpholino (5′-GCCACCATTTTGTTTTTGCTGGAAT-3′) was used as control. zGRK2/3 ATG MO and its 5-bp mismatched morpholino were as in (10). β-Arrestin2 MO was previously described (12). Pol ATG MO was 5′-CTGGGACAAGATGCACATTCTC-CAT-3′. All morpholinos were synthesized by Gene Tools (Philomath, OR). Two nanoliter of the morpholino stock solutions were injected into the yolk of 1–2-cell embryos using a Femtojet microinjector (Eppendorf, Fremont, CA). Morpholino Stock solutions were: 0.5 mM (final dose of 8 ng/embryo) Gas8 and its control MOs, 0.05 mM GRK2 and its control MOs, 0.25 mM Pol and β-arrestin2 MOs. Capped mRNAs for injections were generated using the T7 and SP6 message machine kit (Ambion) using linearized and purified cDNA as the template. Mutagenesis of the morpholino binding site was performed using the QuickChange site-directed mutagenesis kit (Stratagene, Cedar Creek, TX). For rescue experiments, 100 pg mRNA of a mutant *Gas8* mRNA or the *dnPKA* mRNA was co-injected with the indicated morpholino. Injected embryos were kept at 28 °C. 0.003% 1-phenyl-2-thiourea (PTU, Sigma) was added to suppress pigmentation. Embryos were dechorionated prior to their analysis.

Whole Mount in Situ Hybridization and Immunofluorescence—*In situ* hybridization was performed following standard protocols, with one of the DIG-labeled probes for *Nkx2.2, Pax2*, and *Shh*. Embryos were fixed with 4% paraformaldehyde, digested with proteinase K, and hybridized with the probe at 70 °C. Alkaline phosphatase-conjugated anti-digoxigenin antibody (Roche) was used to detect the signals. After staining with BM purple substrate (Roche), embryos were re-fixed with 4% paraformaldehyde supplemented with 10 mM EDTA and stored in PBS buffer. For imaging, embryos were photographed using a Leica microscope with a plan Apo 1× lens equipped with a Retiga Exi Fast CCD camera (QImaging). For Immunofluorescence, embryos were fixed 27 (for muscle phenotypes, Figs. 6 and 7) or 30 hpf (for cilia analysis, Fig. 8), blocked and incubated overnight with the appropriate primary antibody in blocking solution at 4 °C. The blocking solution included 2% NGS, 1% BSA, 0.1% Fish skin gelatin (Sigma), 0.1% Triton X-100, 0.05% Tween-20, and 0.05% sodium azide in 1× PBS. The next day, the embryos were washed and incubated with a secondary antibody overnight at 4 °C. The 4d9 antibody (1:100), which recognizes the *engrailed* protein in the nuclei of muscle pioneer cells was a kind gift from N. Patel (University of California, Berkeley, CA; Ref. 22). The Prox1 antibody (1:500, Millipore, Temecula, CA) was used to label the nuclei of slow muscle fibers and the acetylated tubulin antibody (1:500, Sigma) was used to label cilia in the zebrafish neural tube. Fluorescent secondary antibodies were used for detection. Stained embryos were deyolked using forceps and flat mounted on slides with Vectashield Hard Set mounting medium (Vector Laboratories, Burlingame, CA). Imaging was performed using a Zeiss LSM510 confocal microscopy system.

Statistical analysis was performed using both Excel and GraphPad Prism software (San Diego, CA). *p* values were calculated by either two tailed Student's t-test or one way Anova with Bonferroni's post hoc test for multiple group comparison as indicated in the text. Prior to each t-test, an f-test was applied to determine whether the variances are significantly different.

RESULTS

Gas8 Is a Smo-binding Protein—To identify novel Smo-binding proteins we have applied a yeast two-hybrid screen using the last 211 residues of human Smo C terminus as bait. Several potential partner proteins from a human cDNA library enabled the survival of yeast clones expressing human Smo C terminus. Of these, Gas8 appeared in four cDNA fragments; one containing the last 93 residues of Gas8 while the other 3 clones included the last 122 residues. To confirm this potential interaction we first repeated the two-hybrid assay in yeast using the same bait, but with 2 versions of Gas8 cDNA as a prey, either encoding

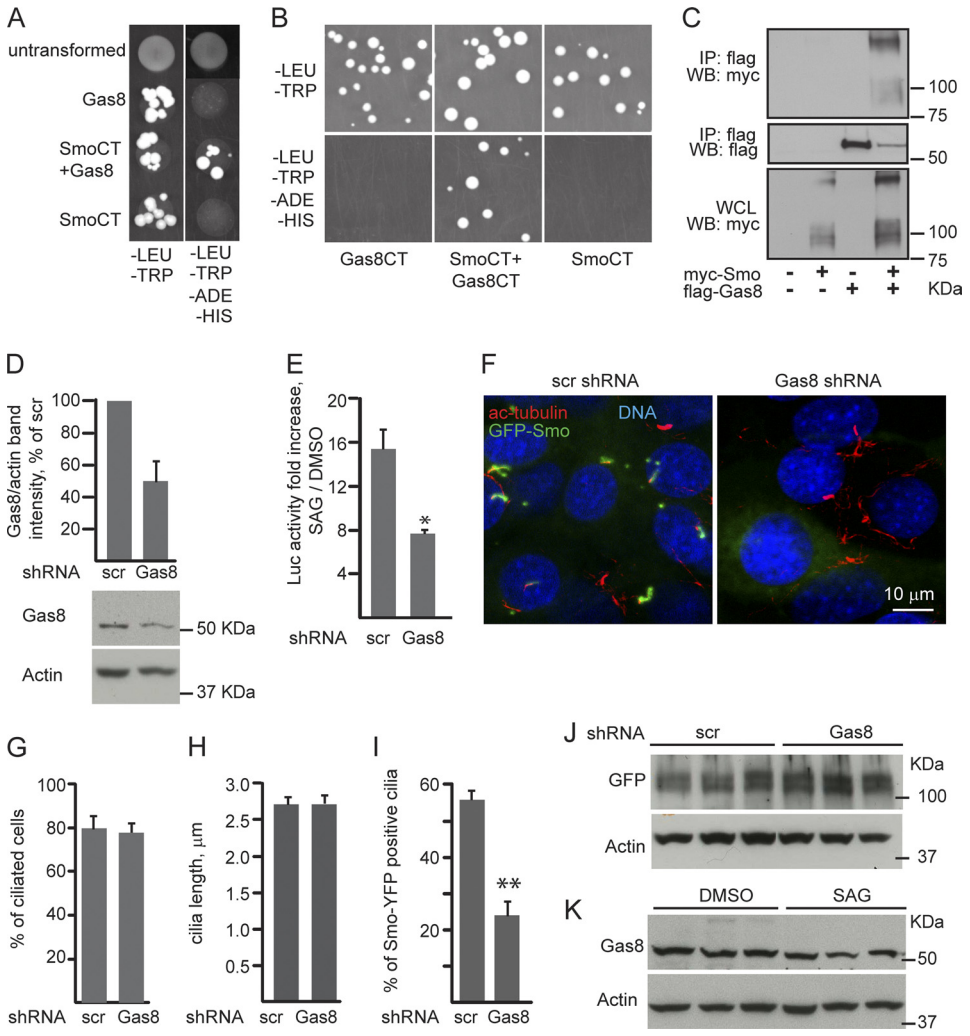

FIGURE 1. **Gas8 is important for Smo signaling and cilary localization.** *A* and *B*, association between Smo and Gas8 was assayed *in vitro* by yeast two-hybrid technique using the last 211 residues of human Smo as a bait (*SmoCT*) and Gas8 cDNA as prey, either encoding Gas8 residues 357–478 (Gas8, *A*) or its 93 C-terminal residues (Gas8CT, *B*) under screening conditions lacking histidine and adenine (*-HIS*, *-ADE*). *C*, Smo and Gas8 specifically interact in HEK cells. HEK cells were transiently transfected with pcDNA3.1 control vector, Myc-tagged Smo, Flag-tagged mouse Gas8, or both Myc-Smo and Gas8. Lysates were immunoprecipitated (*IP*) with an antibody directed to the Flag tag and immunoblotted for the presence of Myc-Smo or the Flag-tag, *WCL*, whole cell lysate. *D–K*, lentiviral shRNA-mediated Gas8 knock down. *D*, Gas8 protein levels were detected in lysates from NIH-3T3 cells stable for either Gas8 shRNA or a scramble control (scr) shRNA. Anti-actin antibody was used for loading control. Averages ± S.E. were calculated from 4 experiments and presented as percent of scr control. *E*, shRNA stable cell lines were transiently transfected with a Gli luciferase reporter and Renilla luciferase internal control. Cells were treated with either SAG or DMSO for 24 h and then starved overnight in the induction media and lysed. Averaged fold induction in luciferase activity values ± S.E. (SAG/DMSO) were calculated. *, $p < 0.05$. *F*, GFP-Smo cell line was infected with the lentiviral shRNAs to generate double stable lines, plated, and stained for acetylated tubulin (*red*). *G–I*, percent of cells with cilia (*G*), the averaged length of the cilia (*H*), and the percent of GFP-Smo containing cilia (*I*) ± S.E. were calculated from four experiments in GFP-Smo cells stable for either Gas8 or scr shRNAs. **, $p < 0.01$. *J*, GFP-Smo protein levels were detected in the double stable cell lines using an antibody against GFP. *K*, Gas8 protein levels were detected upon scr shRNA following stimulation with SAG or DMSO. In both *J* and *K*, anti-actin antibody was used for loading control. All *p* values were calculated by two-tailed Student's *t* test.

Gas8 residues 357–478 (Gas8, Fig. 1*A*) or a shorter C terminus, harboring the last 93 residues (Gas8CT in Fig. 1*B*). Under our screening conditions, only yeast expressing both Smo C terminus (SmoCT) and one of the 2 Gas8 polypeptides yielded positive colonies (Fig. 1*A* and *B*). We further tested Gas8 and Smo interaction by immunoprecipitation assays in lysates from HEK293 cells, expressing Myc-tagged Smo and Flag-tagged Gas8 constructs. An antibody targeted to the Flag tag co-immunoprecipitated Myc-Smo only when both proteins were co-expressed, indicating a selective interaction between Smo and Gas8 (Fig. 1*C*).

Gas8 Is Important for Shh Signaling and Smo Ciliary Localization—To assess whether the interaction between Gas8 and Smo is functional, we analyzed Gas8 loss of function in NIH-3T3 cells by lentiviral shRNA-mediated knockdown which yielded 50% reduction in Gas8 protein levels (Fig. 1*D*). We examined the Gli-dependent transcriptional activity upon Gas8 knockdown using Gli-dependent luciferase reporter assay (13). We found that SAG stimulation leads to a 15-fold induction in the reporter activity levels in the control scramble (scr) shRNA, while Gas8 shRNA significantly reduced the reporter activities by ~50% (7.7-fold induction, Fig. 1*E*). There was no significant change in Gas8 protein levels in the control cells under SAG treatment, indicating that it is not controlled by Shh pathway (Fig. 1*K*). Gas8 has been previously shown to co-localize with the microtubule organizing center (MTOC), centrosomes and the Golgi apparatus. In ciliated cells, Gas8 is localized to the basal body of the cilia (20). To assess whether Gas8 knockdown interferes with Smo accumulation in the cilia, we

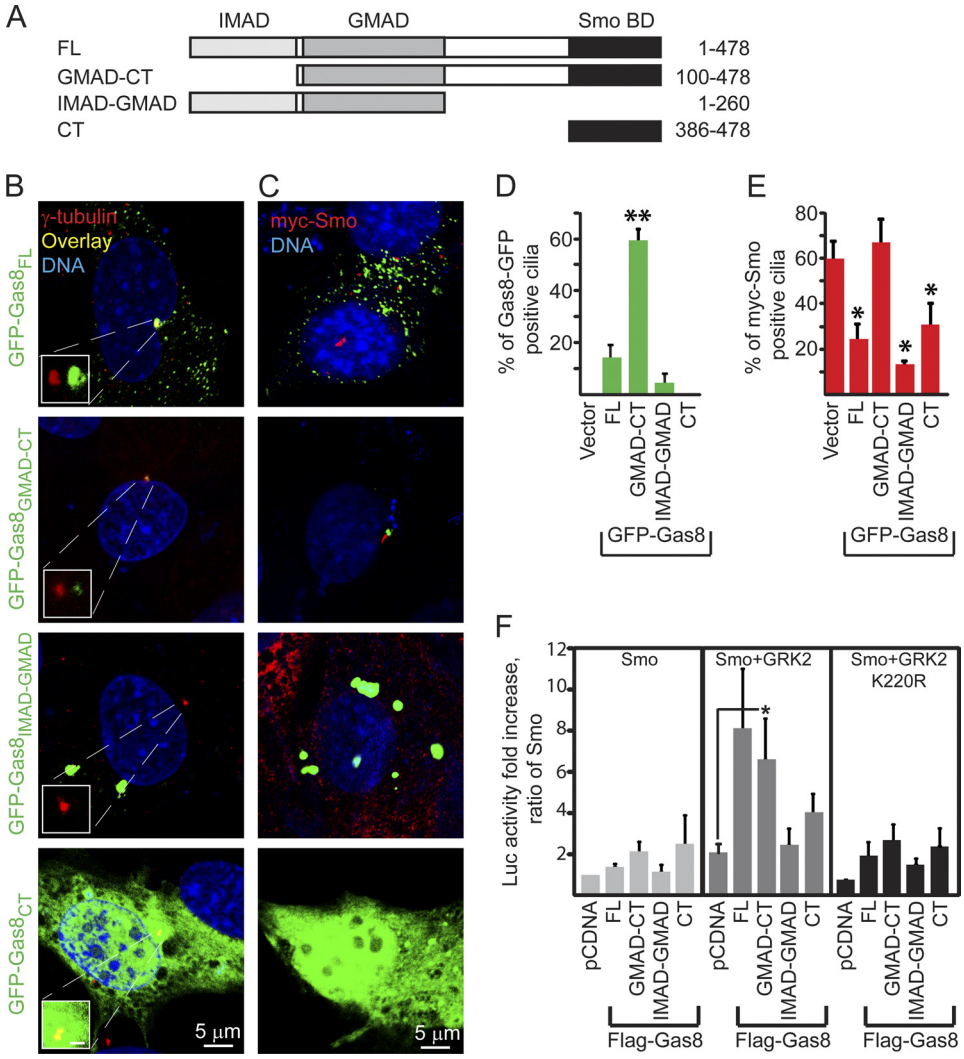

FIGURE 2. **Gas8 polypeptides display differential subcellular localization and exert various effects on Smo ciliary accumulation and activity.** *A*, schematic representation of the recombinant Gas8 polypeptides that were fused to GFP or Flag tag. *B*, C3H10T1/2 cells were transiently transfected with one of the four Gas8-GFP fusion constructs, fixed 72 h post transfection and immunostained using anti γ-tubulin (*red*), which marks the cilia basal body. *Insets* show a magnified shifted overlay of the basal body area. Scale in *insets* is 5 μm. *C*, C3H10T1/2 cells stably expressing Myc-Smo were transfected with one of the four Gas8-GFP fusion constructs, fixed 48 h post-transfection and immunostained using an antibody against the Myc tag (*red*). *Bar graphs* in *D* indicate the averaged percent of GFP-positive cells in *C* that displayed GFP-positive cilia basal body. **, $p = 0.0001$, One-way ANOVA with Bonferroni's post hoc test indicating that $Gas8_{GMAD-CT}$ is different from all other groups. Bar graphs in *E* indicate the averaged percent of GFP-positive cells in *C* that contained Myc-Smo within the cilia shaft. *, $p < 0.05$, two tailed Student's *t*-test as compared with the empty GFP vector group. Averages ± S.E. in *D* and *E* were calculated from three independent experiments. *F*, effect of different Gas8 polypeptides on Gli luciferase reporter activity. C3H10T1/2 cells were transiently transfected with a Gli luciferase reporter, a β-Gal transfection control and the indicated recombinant Flag-tagged Gas8 expression plasmids along with Smo, Smo+GRK2 or Smo+K220R plasmids. Fold increase refers to the increase in luciferase activity relative to a sample containing the reporter, Smo and the empty vector pcDNA3.1 ($n = 6$–9 independent experiments for Smo and Smo+GRK2 and 3 for Smo+K220R; *, $p < 0.05$, two tailed Student's *t*-test).

followed Smo subcellular localization in GFP-Smo cells (13) upon stable infection of Gas8 shRNA. Gas8 shRNA does not affect cilia formation or elongation as the percent of ciliated cells and the averaged length of the cilia remain the same (Fig. 1, *F–H*). Consistent with a previous report (13), 56% of the cilia in the control (scr) cells contain GFP-Smo, even without ligand stimulation (Fig. 1, *F* and *I*). However, upon Gas8 shRNA, only 24% of the cilia contain GFP-Smo, suggesting a role for Gas8 in Smo transport to the cilia. This loss of Smo in the cilia is not due to reduced expression levels of GFP-Smo because similar protein levels were detected upon Gas8 shRNA (Fig. 1*J*).

$Gas8_{GMAD-CT}$ Localization to the Cilia Basal Body Is Associated with Smo Ciliary Localization—To assess which domain of Gas8 is important for its effect on Smo and to tests whether altering the ability of Gas8 to interact with microtubules results in differential effect on Smo signaling we generated four different Flag- or GFP-tagged Gas8 fusion proteins consisting of the different mouse (m)Gas8 domains initially described in Bekker *et al.* (17) and illustrated in Fig. 2*A*: $mGas8_{1-478}$ (full-length, $Gas8_{FL}$), $mGas8_{100-478}$ ($Gas8_{GMAD-CT}$), $mGas8_{1-260}$ ($Gas8_{IMAD-GMAD}$), and $mGas8_{386-478}$ ($Gas8_{CT}$). The last construct consists of the 93 amino acids that bind Smo C terminus and is shorter than the C-terminal construct designed by Bekker *et al.* (17). We followed the subcellular localization of GFP tagged-mGas8 fusion proteins in C3H10T1/2 cells, which we have previously used to monitor Smo-dependent signaling (11). The majority of GFP-$Gas8_{FL}$-expressing cells display a punctated cytoplasmic distribution of $Gas8_{FL}$, probably in vesicles

along cellular microtubules (Fig. 2*B* and supplemental Fig. S1, *left panels*). A smaller fraction (15–20%) of $Gas8_{FL}$ is localized to the basal body of the cilia in addition to its localization in vesicles. $Gas8_{GMAD\text{-}CT}$ that lacks the N-terminal IMAD sequence is co-localized with γ-tubulin in the cilia basal body of the majority of the transfected cells (Fig. 2*B* and supplemental Fig. S1). The observation that only a small fraction of $Gas8_{FL}$ is distributed to the cilia basal body could reflect a weak and transient binding to microtubules (17). Interestingly, $Gas8_{CT}$ and the truncated $Gas8_{IMAD\text{-}GMAD}$ constructs are not associated with microtubules, but accumulate in the cytoplasm or in aggregates, respectively. Using markers for the Golgi apparatus (GM130) and lysosomes (LysoTracker), we found that $Gas8_{IMAD\text{-}GMAD}$ aggregates are not co-localized to either of these organelles, although they are found in proximity to the Golgi (supplemental Fig. S2). To test which of Gas8 domains supports changes in Smo subcellular localization, we transfected C3H10T1/2 cells, which stably express Myc-Smo with the different GFP-Gas8 constructs. Smo in those cells is constitutively active (11) and accumulates in the cilia (Fig. 2, *C* and *E*). The accumulation of $Gas8_{GMAD\text{-}CT}$ in the cilia basal body does not affect the percent of Smo positive cilia (Fig. 2, *C–E*). However, all other forms of Gas8 that do not accumulate in proximity to the cilia basal body prevent Smo ciliary localization ($Gas8_{FL}$, $Gas8_{IMAD\text{-}GMAD}$, and $Gas8_{CT}$ in Fig. 2, *C–E*), suggesting a role for the GMAD-CT domain in Smo targeting to the cilia.

Gas8 Stimulation of Smo Activity in Cells Is Dependent of Gas8 C Terminus and GRK2—To asses which domain of Gas8 is important for its effect on Smo-dependent signaling we have transiently transfected C3H10T1/2 with the different Flag-tagged Gas8 fusion proteins and measured Gli-dependent luciferase reporter activities. Because GRK2 enhances Smo-mediated transcriptional activity in cells (10, 11), we measured the reporter activity following co-transfection of Myc-Smo, Gas8, and GRK2. As expected, GRK2 and Myc-Smo induced a 2-fold increase in the reporter activity as compared with Myc-Smo alone (Fig. 2*F*). In the presence of GRK2, $Gas8_{GMAD\text{-}CT}$ induced a statistically significant 3-fold increase in activity (Fig. 2*F*, *, $p < 0.05$, two tailed Student's t-test). However, the effect of $Gas8_{FL}$ on the reporter activity was highly variable and thus did not reach statistical significance. No significant induction was observed either in the absence of GRK2 or with the kinase dead GRK2 mutant (GRK2 K220R, Ref. 23) as well as following co-transfection of GRK2 and either $Gas8_{IMAD\text{-}GMAD}$ or $Gas8_{CT}$. These findings suggest that GRK2 and $Gas8_{GMAD\text{-}CT}$ potentially cooperate to activate Gli-dependent transcription in the presence of Smo.

Catalytically Active GRK2 Facilitates Cilia Elongation and Smo Accumulation in Cilia—Earlier reports showed that GRK2 can phosphorylate both tubulin and Smo (9, 10). Given the GRK2-dependent effects of Gas8 on Smo signaling, we sought to examine whether GRK2 is involved in targeting Smo to ciliary microtubules. We studied cilia from 4 lines of C3H10T1/2 cells stably transfected with GRK2, Myc-Smo, Myc-Smo with GRK2 (Smo_GRK2) or Myc-Smo with GRK2 K220R (Smo_K220R, (11)). Surprisingly, Smo_GRK2 stable cells assemble 2.2-fold longer cilia as compared with GRK2 or Smo alone and visualized by acetylated tubulin staining (Fig. 3, *A* and *C*). This structural change is accompanied by an induction of Gli activity, which can be blocked by the Smo antagonist cyclopamine (Fig. 3*E* and Ref. 11). Cilia from GRK2 or Smo cells are indistinguishable from cilia of cells expressing empty vectors only (Fig. 3, *A* and *C*). Moreover, cilia from Smo_K220R cells were similar to those of Smo cells, suggesting that the kinase activity of GRK2 is important for its effect on cilia elongation. Population distribution analysis further confirms the shift in cilia length in our Smo_GRK2 cell line (supplemental Fig. S3). We hypothesized that in the presence of GRK2 and Smo, longer cilia may allow more Smo to accumulate within the cilia and that this accumulation may contribute to the observed higher transcriptional activity levels. Indeed, we found that cilia which are positive for Myc-Smo were significantly longer in the Smo_GRK2 line as compared with Smo and Smo_K220R lines (Fig. 3, *A* and *C*). In those positive cilia, Smo was found along the cilium shaft and at the distal tip (Fig. 3*A*, *insets*). However, GRK2 showed cytoplasmic localization (Fig. 3*B*). The ratio between the length of cilia that are positive for Myc-Smo and the length of cilia labeled with acetylated tubulin was similar among the different cell lines (80–90% of the cilium shaft is filled with Myc-Smo, Fig. 3). Moreover, the staining intensity of Myc-Smo signal was also unchanged (Fig. 3*D*), suggesting that Smo accumulation within cilia is proportional to the increased length of the cilium, an effect that is GRK2-dependent.

Gas8 Regulates Zebrafish Early Development and Hh Target Gene Expression—Loss of zebrafish (z)Gas8 leads to various developmental abnormalities, including hydrocephaly, disorganized somites, pericardial edema, left-right asymmetry, and abnormal ear development (14). Given that regulated Hh signaling is essential for normal inner ear development in zebrafish (24) and based on the interaction between Smo and Gas8, we hypothesized that at least some of the reported abnormalities may be associated with disrupted Hh signaling pathway. Thus, we injected fertilized zebrafish eggs with a translation blocking morpholino against zGas8 (Gas8 MO) or its control morpholino which lacks the ability to bind Gas8 mRNA due to 5 point mutations (Gas8 CT MO). As is shown in Fig. 4*A* and *E*, 189/269 Gas8 morphant embryos displayed phenotypes including pericardial edema, misshaped somites and hydrocephaly, while 128/171 embryos injected with the control morpholino developed normally. We examined the expression levels of the Hh-target genes Nkx2.2 (25) and Pax2 (24) using whole embryo *in situ* hybridization at 24 hpf. We detected down-regulation of *Nkx2.2* in the hind brain (hb) and floor plate (fp) of 152/213 Gas8 morphants (Fig. 4, *B* and *F*) and a decrease of *Pax2* in the otic vesicle (ov) of 166/231 morphants (Fig. 4, *C* and *G*) as compared with non-injected and control embryos. *Shh* mRNA levels were unaffected in 73/79 embryos injected with Gas8 MO, indicating that the reduction in Hh target gene transcripts is not due to an upstream reduction in Shh ligand (Fig. 4, *D* and *H*). Normal embryonic development was rescued in 54/91 embryos co-injected with 100 pg z*Gas8* mRNA bearing six silent mutations in the MO binding site (Fig. 4, *A* and *E*). Moreover, *Nkx2.2* and *Pax2* expression levels were rescued by co-injection of z*Gas8* mRNA in 67/93 and 51/72 injected embryos, respectively. Co-injection of a dominant negative ver-

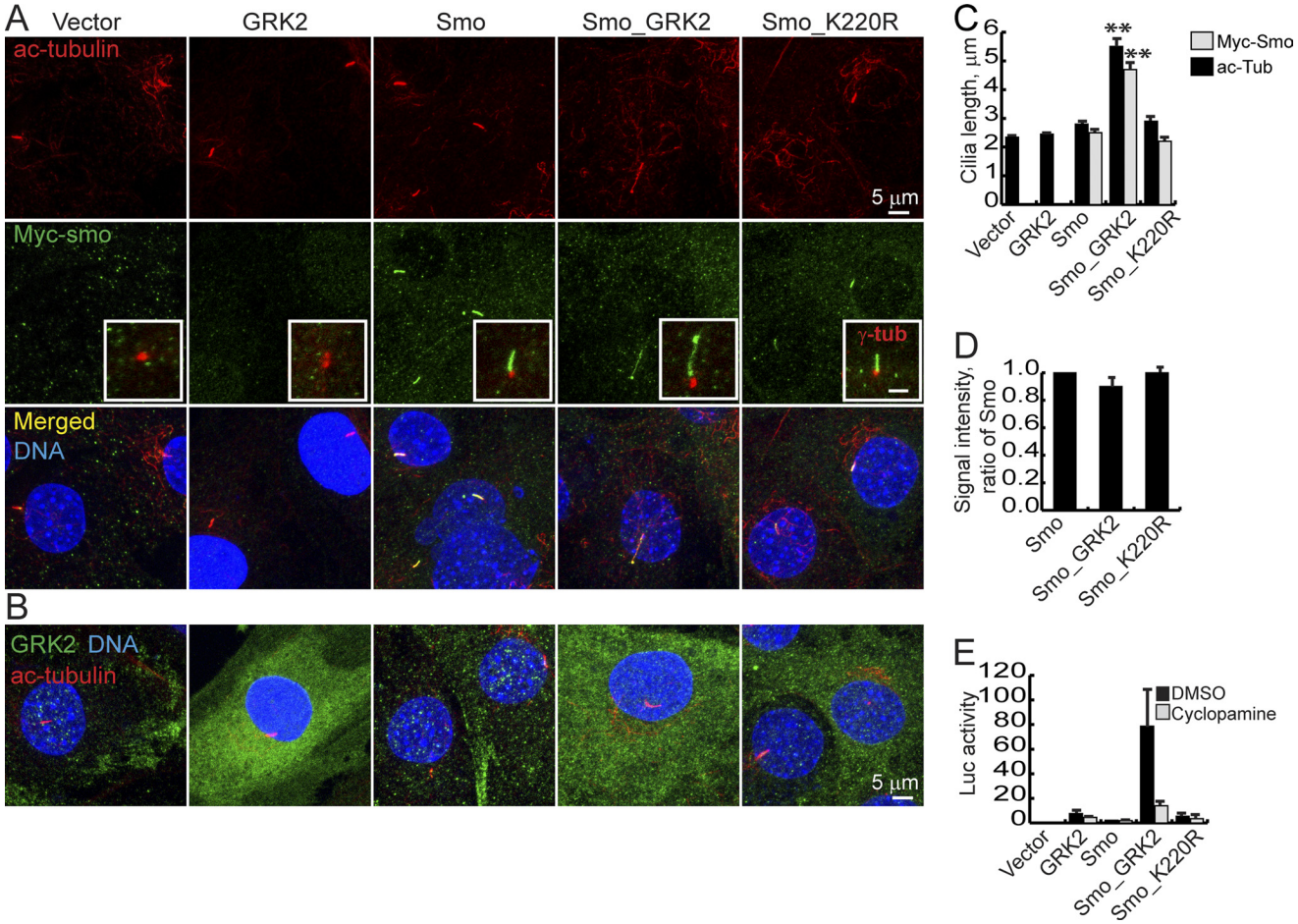

FIGURE 3. **Stable transfection of GRK2 modifies ciliary structure and Smo accumulation.** *A*, cilia of C3H10T1/2 cells stably expressing GRK2, Myc-tagged Smo (Smo), Myc-tagged Smo, and GRK2 (Smo_GRK2), Myc-tagged Smo and the kinase dead GRK2 (Smo_K220R) or two empty vectors were labeled using antibodies against acetylated tubulin (*A*, *upper panel*) and the Myc tag (*A*, *middle panel*, merged images in the *bottom panel*). *Insets* in *A* show co-staining of γ-tubulin (*red*) and anti Myc (*green*). The *inset's* scale is 2 μm. In *B*, GRK2 and acetylated tubulin co-staining show that GRK2 is not enriched within the cilia. *C*. averages ± S.E. of general cilia length and Myc-Smo positive cilia length, calculated from three samples per indicated cell line and 50–100 cilia analyzed in each sample. **, $p < 0.001$, Student's *t*-test. *D*, averages ± S.E. of Myc-Smo staining intensities in the cilia analyzed in *C* and displayed as a ratio of Smo. All measurements were done on confocal Z stacks. *E*, C3H10T1/2 cells stably expressing the indicated proteins were transfected with the Gli reporter and a β-gal transfection control, treated as indicated and assayed for luciferase activity 72 h post-transfection.

sion of PKA (*dnPKA*) mRNA, which has been previously shown to induce constitutive activation of Hh at the level of Gli (26), reversed both the phenotype (Fig. 4, *A* and *E*, 33/56 embryos developed normally) and the attenuated expression of Hh target genes that were caused by zGas8 inhibition (Fig. 4, *B*, *C*, *F*, and *G*, 34/56 and 38/53 embryos displayed unaffected *Nkx2.2* and *Pax2* mRNA levels, respectively).

To assess the severity of Gas8 MO effects we compared Gas8 morphants to Smo^{s294} mutant fish, where the Smo gene is mutated (21) and to fish injected with 2 other MOs targeting either β-arrestin2 or Polaris (Pol/Tg737/IFT88), an anterograde IFT protein important for cilia formation (27). Already at 24 hpf, Gas8 morphants showed similar, although less severe phenotypes like those observed in β-arrestin2 morphants and Smo^{s294} mutant fish (Fig. 5, *C* as compared with *D* and *E*). Interestingly, those phenotypes seem to be stronger than in Pol morphants at 24 hpf, but milder at 72 hpf (Fig. 5*F*). The observed down-regulation of *Nkx2.2* and *Pax2* mRNAs following Gas8 knockdown is similar to their attenuated expression in β-arrestin2 morphants (Fig. 5, *I* and *O* as compared with Fig. 5, *J* and *P*) but only partially similar to Pol morphants, which had normal *Nkx2.2* levels (Fig. 5*L*). Smo^{s294} mutant displayed more dramatic reduction in both mRNAs, consistent with severe impairment of the Hh pathway (Fig. 5, *K* and *Q*). These findings suggest a selective but moderate attenuation of Hh signaling in embryos with reduced zGas8 expression.

zGas8 and GRK2/3 Knockdown Display a Synergistic Effect on Slow Muscle Development—Hh signaling pathway is critical for the development of slow muscle fibers in zebrafish (28, 29). Interfering with the Hh signaling using GRK2/3 and β-arrestin2 MOs lead to impaired development of slow muscles (10, 12). Given the effects of Gas8 MO on Hh target gene expression during development, we analyzed the expression of slow muscle markers in Gas8 morphants. Depletion of Gas8 reduced the number of *Prox1*+ slow muscle cells (Fig. 6, *B* and *G*) and *engrailed*+ muscle pioneer cells (Fig. 6, *B* and *H*) as assessed by whole mount immunofluorescence. This perturbed muscle development is similar to the effect of GRK2/3 (Ref. 10 and Fig. 7*C*) and β-arrestin2 MOs (Fig. 6*D* and Ref. 12) but is more subtle when compared with Smo^{s294} mutants, where muscle pioneer cells are completely absent (Fig. 6, *F–H*). However, the reduction in muscle pioneer cells in Gas8 morphants is stronger

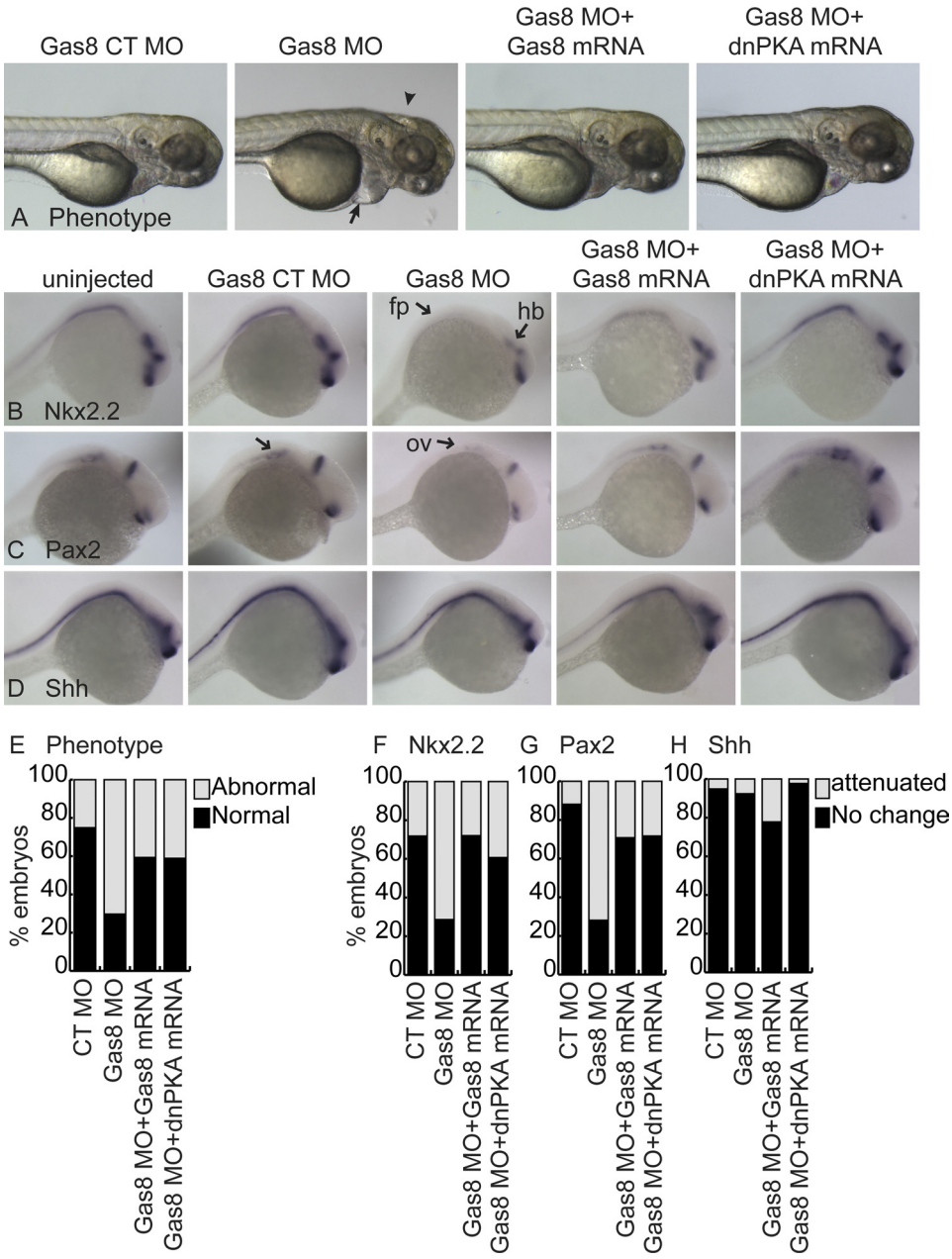

FIGURE 4. **zGas8 is important for early development and proper Hh signaling.** *A*, zebrafish embryos injected with Gas8 MO displayed pericardial edema (*arrow*), hydrocephaly (*arrowhead*) and misshaped somites. These phenotypes can be rescued by the co-injection of a MO-resistant *zGas8* mRNA and by *dnPKA* mRNA. Gas8 control MO (Gas8 CT MO) injected embryos were indistinguishable from the non-injected wildtype embryos (see also Fig. 5). 72 hpf embryos are shown laterally. *B–D*, whole mount *in situ* hybridization of *Nkx2.2* (*B*), *Pax2* (*C*), and *Shh* (*D*), showing attenuated *Nkx2.2* expression in the floor plate (*fp*) and hind brain (*hb*), and *Pax2* in the otic vesicle (*ov*) of 24 hpf embryos injected with Gas8 MO, but not with its CT MO. Normal expression levels achieved by co-injection of *zGas8* or *dnPKA* mRNAs. *Shh* expression levels remained similar under all conditions. *E–H*, stacked bar graph analysis of the percentage of embryos with normal or abnormal phenotype (*E*), and the percentage of embryos that displayed attenuation or no change in the indicated transcript levels (*F–H*) following the different injections. Stacked bar graphs summarize at least 4 separate injections of Gas8 MO and their controls. Two of these experiments included *zGas8* mRNA and the other two included *dnPKA* mRNA for rescue. Numbers of injected embryos are indicated in the text.

than in Pol morphant embryos (Fig. 6, *E*, *G*, and *H*). The numbers of both slow muscle and muscle pioneer cells were rescued by the co-injection of Gas8 MO and dnPKA mRNA (Fig. 6, *C*, *G*, and *H*). Moreover, Consistently with our finding that Gas8 and GRK2 cooperate to induce Smo-dependent signaling in cells, co-injection of Gas8 MO and GRK2/3 MO synergistically decreased the number of muscle pioneer cells as compared with separate injections of the two MOs (Fig. 7, *E versus B* and *C* and bar graph in Fig. 7*G*).

zGas8 and zGRK2/3 Regulate Hh Signaling but Are Not Essential for Cilia Assembly in Zebrafish—To determine whether Gas8 and GRK2/3 function in the same pathway, we co-injected GRK2/3 MO and z*Gas8* mRNA and then examined *Nkx2.2* expression levels. As previously reported (10), GRK2/3 MO caused a moderate reduction of *Nkx2.2* mRNA in the developing brain of 46/60 zebrafish embryos 24 h post injection (Fig. 8*B*) as compared with 5/35 embryos injected with its control MO (Fig. 8*A*). *Nkx2.2* expression levels were rescued in

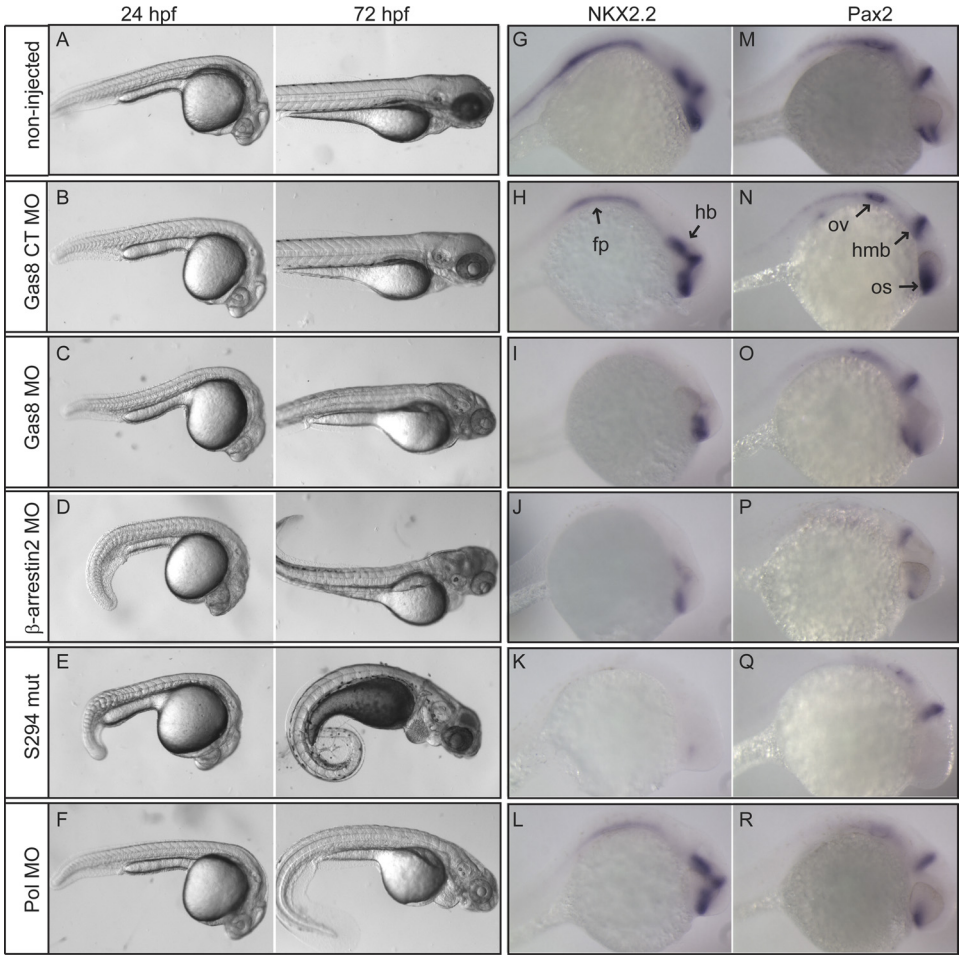

FIGURE 5. **Comparison between Gas8 morphants, β-arrestin2 and Pol morphants as well as Hh mutants.** Zebrafish embryos injected with the indicated MO as well as non injected wild type and Smo^{S294} mutants were either photographed 24 and 72 hpf (*A–F*) or subjected to whole mount *in situ* hybridization 24 hpf (*G–R*). Embryos injected with Gas8 MO display mild developmental abnormalities (*C*) as compared with embryos injected with β-arrestin MO (*D*) or Smo^{S294} mutants (*E*), which display curled body and disorganized somites at 24 and 72 hpf. Embryos injected with Pol MO (*F*) show severely curved body and disorganized somites only at 72 hpf. Control MO (*B*, Gas8 CT MO) injected embryos are indistinguishable from non injected wt (*A*). *G–R*, whole embryo *in situ* hybridization shows attenuated *Nkx2.2* expression in the floor plate (*fp*) and hind brain (*hb*), and *Pax2* in the otic vesicle (*ov*) of 24 hpf embryos injected with Gas8 MO (*I*, *O*), similar to the attenuated transcription of both transcripts following β-arrestin2 MO injection (*J*, *P*). Pol MO injection leads to declined *Pax2* (*R*) but not *Nkx2.2* (*L*) expression. Both transcripts are dramatically reduced in Smo^{S294} mutants (*K*, *Q*). *Pax2* is diminished in Smo^{S294} optic stalk (*os*).

36/53 GRK2/3 morphants by the co-injection of *zGas8* mRNA (Fig. 8*D*), suggesting a genetic interaction between Gas8 and GRK2/3. *zGas8* mRNA did not affect *Nkx2.2* levels in 33/38 control embryos (Fig. 8*C*). Given the effect of GRK2/3 on cilia elongation, we explored whether Gas8 or GRK2/3 MOs can affect cilia formation in vertebrates. Acetylated tubulin staining 30 hpf revealed that Pol MO reduces the numbers of cilia in the caudal neural tube, while neither Gas8 nor GRK2/3 MOs affect cilia numbers or architecture, suggesting that both proteins are not required for ciliogenesis in zebrafish (Fig. 8*F*).

DISCUSSION

In this study, using gain and loss of function approaches, we identified Gas8 as a novel interacting partner of Smo that cooperates with GRK2 and thus promotes Smo signaling *in vitro* and *in vivo*.

Previously, Gas8 has been suggested to serve as a linker between the DRC and microtubules through its GMAD domain, regulating dynein and microtubule sliding in motile cilia and flagella (16, 17, 20, 30). We show here that 50% reduction in Gas8 protein levels is sufficient to attenuate Smo-dependent signaling and leads to the loss of Smo within the cilia without affecting ciliogenesis. We also find that altering the ability of Gas8 to interact with microtubules results in differential effect on Smo signaling. $mGas8_{GMAD\text{-}CT}$ accumulates in the cilium basal body and induces Smo signaling in cells in a GRK2 dependent manner. Truncated forms of Gas8 that do not localize to the cilium decrease Smo ciliary accumulation and are unable to increase signaling. However, the full-length Gas8 could be detected both at the base of the cilia and in vesicles in the cytoplasm, which may explain the high variability in the levels of Smo stimulation as compared with the induction achieved by the removal of IMAD from the expression vector. This may also indicate that the IMAD has to be sequestered to allow maximal interaction with microtubules as was previously suggested (17).

Whereas Gas8 knockdown in ciliated cells and zebrafish embryos is sufficient for moderately attenuating Hh signaling, its stimulatory effect on activity depends on GRK2 being catalytically active. The mechanism of this dependence is not clear,

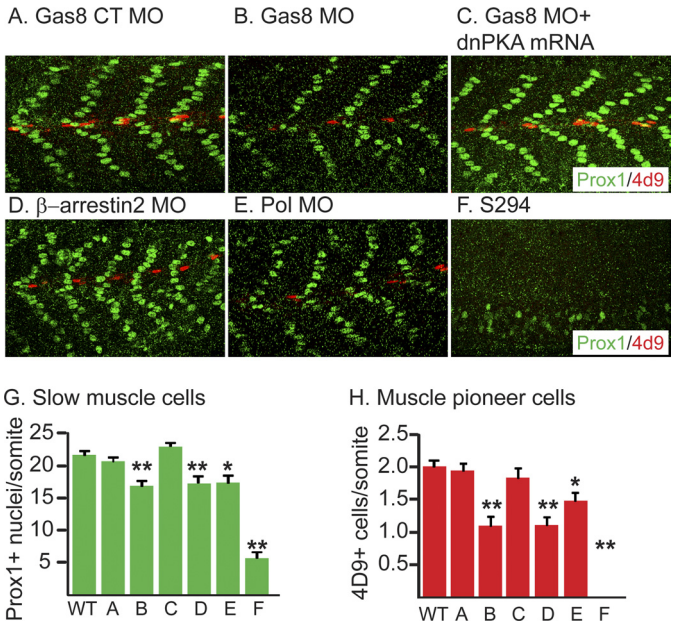

FIGURE 6. **Gas8 morphants show slow muscle defects.** Analysis of slow muscle cell nuclei (Prox1, *green*) and *engrailed*+ muscle pioneer cells (4d9, *red*) in 27 hpf embyos injected with Gas8 CT MO (*A*), Gas8 MO (*B*), Gas8 MO, and dnPKA mRNA co-injection (*C*), β-arrestin2 MO (*D*), Pol MO (*E*) as well as Smo^{S294} mutants (*F*). *G* and *H*, bargraphs represent numbers of *Prox1*+ cells (*G*) and *engrailed*+ cells (*H*) ± S.E. measured in several somites of at least 9 embryos in each condition. Gas8 MO leads to a reduction in both slow muscle cells and muscle pioneer cells (*B*, *G*, and *H*), similar to the effect of β-arrestin2 MO. The phenotype is milder than in Smo^{S294} mutant somites and it could be fully rescued by dnPKA mRNA. Embryos are shown in lateral view, anterior to the left. *, $p < 0.05$; **, $p < 0.01$, two-tailed Student's *t*-test compared with the non-injected wt.

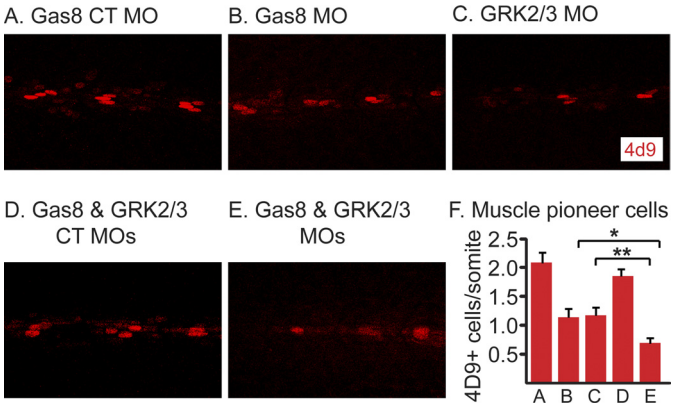

FIGURE 7. **A synergistic effect of Gas8 and GRK2/3 knockdown on muscle pioneer cells.** Analysis of slow muscle cell nuclei (Prox1, *green*) and *engrailed*+ muscle pioneer cells (4d9, *red*) in 27 hpf embyos injected with Gas8 CT MO (*A*), Gas8 MO (*B*), GRK2/3 MO (*C*), Gas8 CT MO and GRK2/3 CT MO co-injection (*D*) and Gas8 MO and GRK2/3 MO co-injection (*E*). *F*, bar graphs represent numbers of *engrailed*+ cells ± S.E. measured in several somites. Separate injections of Gas8 MO (*B*, $n = 8$) and GRK2/3 MO (*C*, $n = 7$) lead to a reduction in muscle pioneer cells as compared with Gas8 CT MO (*A*, $n = 8$, $p < 0.01$). Co-injection of Gas8 and GRK2/3 MO (*E*, $n = 11$) leads to an augment of the reduction in muscle pioneer cells as compared with separate injections of either Gas8 MO or GRK2/3 MO (*F*, *, $p < 0.01$; **, $p < 0.05$) as well as compared with co-injection of the two control MOs (*F*, $n = 6$, $p < 0.01$). Embryos are shown in lateral view, anterior to the *left*. *p* values were calculated by two-tailed Student's *t*-test.

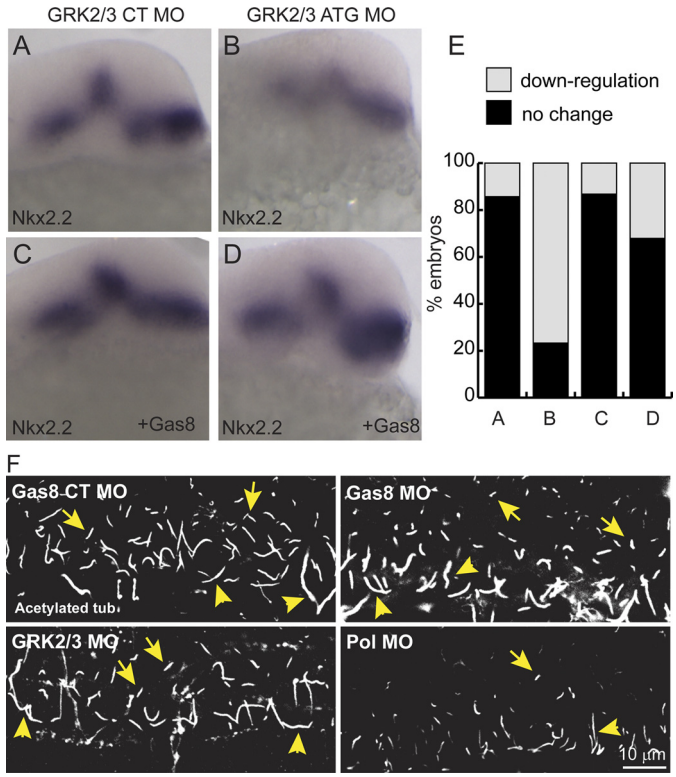

FIGURE 8. *A–E*, zGas8 mRNA reverses GRK2/3 MO effects. Whole mount *in situ* hybridization of *Nkx2.2* show moderate reduction in *Nkx2.2* expression levels 24 h postinjection of GRK2/3 MO (*B*) as compared embryos injected with its control MO (*A*). Co-injection of *zGas8* mRNA normalized *Nkx2.2* expression levels (*D*), but did not affect *Nkx2.2* levels in control embryos (*C*). *E*, percent of injected embryos with the indicated *Nkx2.2* expression levels as compared with wild-type embryos. Embryos are shown in lateral view, anterior to the top. Numbers of embryos from 2 injections are indicated in the text. *F*, zGas8 and zGRK2/3 knockdown does not prevent cilia formation. Zebrafish embryos injected with Gas8 CT MO, Gas8 MO, GRK2/3 MO, or Pol MO were fixed 30 hpf and immunostained with an anti-acetylated tubulin antibody. Both decreases in Gas8 and GRK2/3 did not prevent cilia formation in the zebrafish caudal neural tube, whereas Pol MO yielded a dramatic decrease in cilia numbers ($n = 6–8$ embryos). Embryos are shown laterally, anterior to the *left*. *Yellow arrowheads* indicate motile cilia in the floor plate (*long*). *Yellow arrows* indicate primary cilia more dorsally in the neural tube (*short*).

but it may be partially explained by the structural modification in ciliary length caused by simultaneous expression of GRK2 and Smo in stable cell lines, where higher levels of Smo can be targeted to the cilia. Cilia length is regulated by cAMP levels (31, 32). However, the observation that stable expression of Smo and GRK2 can affect cilia length is consistent with a previous suggestion that the Hh pathway by itself may influence the length of primary cilia (33). Surprisingly, GRK2 does not have to traffic into the cilia or to the basal body in order to exert its effect. Possibly, GRK2 phosphorylates cytoplasmic tubulin or other proteins that would enter the cilium and modulate microtubule organization. Alternatively, recent studies have shown that temporary down-regulation of GRK2 is required for normal cell cycle progression (34) and that depletion of β-arrestin results in uncontrolled cell proliferation and reduced cilia numbers (35), suggesting an indirect mechanism involving cell cycle control. Yet, other mechanisms can certainly not be ruled out.

Our findings suggest a role for Gas8 in vertebrate Hh signaling. Gas8 knockdown in zebrafish results in various developmental abnormalities, including impaired development of slow muscles, a process that depends on Hh signaling (28, 29). Those abnormalities are accompanied by attenuated Hh transcriptional responses, further confirming the involvement of Gas8 in

this pathway. The mild loss of function phenotypes of Gas8 compared with those of Smo^{s294} point to Gas8 as a moderate or transient effector of the Hh pathway that exerts its activity upstream of Gli. The aberrant slow muscle development as well as the attenuation in Hh target gene expression are similar to the effects of both GRK2/3 and β-arrestin2 MOs. Although these comparisons are useful to assess the contribution of Gas8 to the process, they do not necessarily represent the absolute contribution of individual components of the pathway. It is also noteworthy that Gas8 MO effects were relatively stronger than those of the loss of function of the IFT component Polaris. Whereas the requirement of IFT proteins for proper Hh signaling in mice is well documented (36–39), such dependence in zebrafish remains uncertain. A study in zebrafish lacking cilia has suggested a dampening of Hh signaling (40) while another reported no signaling effect in IFT mutant and morphant fish (41). Here, we detected a mild effect of Pol MO on slow muscle development, on *Pax2* expression but no effect on *Nkx2.2*. Given that Gas8 is probably not critical for cilia assembly, we postulate that the effects of Gas8 on Hh signaling are likely mediated by its selective interaction with Smo. However, we cannot rule out the possibility that Gas8 has a role in primary cilia formation, a function that could potentially requires only low levels of Gas8 protein.

Our observations are consistent with the previously proposed model for the cellular function of Gas8 to reversibly inhibit dynein at the basal body of the primary cilium (20). Such transient inhibition may be required for the import of proteins into the cilia. Thus, the interaction between Smo and Gas8 could facilitate the ciliary import of Smo. The potential relationship between Gas8 and GRK2 in Smo signaling should be interesting to investigate further. It is possible that Gas8 and GRK2 cooperate to regulate β-arrestin recruitment to the phosphorylated Smo, resulting in the described interaction of Smo with Kif3A and the consequent anterograde transport of Smo into the cilia (13).

Acknowledgments—We thank Drs. M. Scott (Stanford University), R. H. Crosbie (UCLA), K. Hill (UCLA), N. Patel K. (University of California, Berkeley), K. Poss (Duke University), M. Bagnat (Duke University), A. Ravanelli (Duke University), and T. Oliver (Duke University) for reagents, fish, and technical advice. We also thank J. Burris for zebrafish facility maintenance. We thank Dr. L. Barak for critically reading the manuscript.

REFERENCES

1. Huangfu, D., and Anderson, K. V. (2006) *Development* **133,** 3–14
2. McMahon, A. P., Ingham, P. W., and Tabin, C. J. (2003) *Curr. Top Dev. Biol.* **53,** 1–114
3. Teglund, S., and Toftgård, R. (2010) *Biochim. Biophys. Acta* **1805,** 181–208
4. Goetz, S. C., and Anderson, K. V. (2010) *Nat. Rev. Genet.* **11,** 331–344
5. Wilson, C. W., and Stainier, D. Y. (2010) *BMC Biol.* **8,** 102
6. Chen, W., Ren, X. R., Nelson, C. D., Barak, L. S., Chen, J. K., Beachy, P. A., de Sauvage, F., and Lefkowitz, R. J. (2004) *Science* **306,** 2257–2260
7. Kalderon, D. (2005) *Curr. Biol.* **15,** R175–178
8. Lefkowitz, R. J., and Shenoy, S. K. (2005) *Science* **308,** 512–517
9. Pitcher, J. A., Hall, R. A., Daaka, Y., Zhang, J., Ferguson, S. S., Hester, S., Miller, S., Caron, M. G., Lefkowitz, R. J., and Barak, L. S. (1998) *J. Biol. Chem.* **273,** 12316–12324
10. Philipp, M., Fralish, G. B., Meloni, A. R., Chen, W., MacInnes, A. W., Barak, L. S., and Caron, M. G. (2008) *Mol. Biol. Cell* **19,** 5478–5489
11. Meloni, A. R., Fralish, G. B., Kelly, P., Salahpour, A., Chen, J. K., Wechsler-Reya, R. J., Lefkowitz, R. J., and Caron, M. G. (2006) *Mol. Cell. Biol.* **26,** 7550–7560
12. Wilbanks, A. M., Fralish, G. B., Kirby, M. L., Barak, L. S., Li, Y. X., and Caron, M. G. (2004) *Science* **306,** 2264–2267
13. Kovacs, J. J., Whalen, E. J., Liu, R., Xiao, K., Kim, J., Chen, M., Wang, J., Chen, W., and Lefkowitz, R. J. (2008) *Science* **320,** 1777–1781
14. Colantonio, J. R., Vermot, J., Wu, D., Langenbacher, A. D., Fraser, S., Chen, J. N., and Hill, K. L. (2009) *Nature* **457,** 205–209
15. Hutchings, N. R., Donelson, J. E., and Hill, K. L. (2002) *J. Cell Biol.* **156,** 867–877
16. Rupp, G., and Porter, M. E. (2003) *J. Cell Biol.* **162,** 47–57
17. Bekker, J. M., Colantonio, J. R., Stephens, A. D., Clarke, W. T., King, S. J., Hill, K. L., and Crosbie, R. H. (2007) *Cell Motil. Cytoskeleton* **64,** 461–473
18. Sasaki, H., Hui, C., Nakafuku, M., and Kondoh, H. (1997) *Development* **124,** 1313–1322
19. Barak, L. S., Ferguson, S. S., Zhang, J., and Caron, M. G. (1997) *J. Biol. Chem.* **272,** 27497–27500
20. Colantonio, J. R., Bekker, J. M., Kim, S. J., Morrissey, K. M., Crosbie, R. H., and Hill, K. L. (2006) *Traffic* **7,** 538–548
21. Aanstad, P., Santos, N., Corbit, K. C., Scherz, P. J., Trinh le, A., Salvenmoser, W., Huisken, J., Reiter, J. F., and Stainier, D. Y. (2009) *Curr. Biol.* **19,** 1034–1039
22. Patel, N. H., Martin-Blanco, E., Coleman, K. G., Poole, S. J., Ellis, M. C., Kornberg, T. B., and Goodman, C. S. (1989) *Cell* **58,** 955–968
23. Kong, G., Penn, R., and Benovic, J. L. (1994) *J. Biol. Chem.* **269,** 13084–13087
24. Hammond, K. L., van Eeden, F. J., and Whitfield, T. T. (2010) *Development* **137,** 1361–1371
25. Barth, K. A., and Wilson, S. W. (1995) *Development* **121,** 1755–1768
26. Epstein, D. J., Marti, E., Scott, M. P., and McMahon, A. P. (1996) *Development* **122,** 2885–2894
27. Bisgrove, B. W., Snarr, B. S., Emrazian, A., and Yost, H. J. (2005) *Dev. Biol.* **287,** 274–288
28. Barresi, M. J., Stickney, H. L., and Devoto, S. H. (2000) *Development* **127,** 2189–2199
29. Lewis, K. E., Currie, P. D., Roy, S., Schauerte, H., Haffter, P., and Ingham, P. W. (1999) *Dev. Biol.* **216,** 469–480
30. Heuser, T., Raytchev, M., Krell, J., Porter, M. E., and Nicastro, D. (2009) *J. Cell Biol.* **187,** 921–933
31. Besschetnova, T. Y., Kolpakova-Hart, E., Guan, Y., Zhou, J., Olsen, B. R., and Shah, J. V. (2010) *Curr. Biol.* **20,** 182–187
32. Ou, Y., Ruan, Y., Cheng, M., Moser, J. J., Rattner, J. B., and van der Hoorn, F. A. (2009) *Exp. Cell Res.* **315,** 2802–2817
33. Kim, H. R., Richardson, J., van Eeden, F., and Ingham, P. W. (2010) *BMC Biol* **8,** 65
34. Penela, P., Rivas, V., Salcedo, A., and Mayor, F., Jr. (2010) *Proc. Natl. Acad. Sci. U.S.A.* **107,** 1118–1123
35. Molla-Herman, A., Boularan, C., Ghossoub, R., Scott, M. G., Burtey, A., Zarka, M., Saunier, S., Concordet, J. P., Marullo, S., and Benmerah, A. (2008) *PLoS ONE* **3,** e3728
36. Haycraft, C. J., Banizs, B., Aydin-Son, Y., Zhang, Q., Michaud, E. J., and Yoder, B. K. (2005) *PLoS Genet* **1,** e53
37. Huangfu, D., and Anderson, K. V. (2005) *Proc. Natl. Acad. Sci. U.S.A.* **102,** 11325–11330
38. Huangfu, D., Liu, A., Rakeman, A. S., Murcia, N. S., Niswander, L., and Anderson, K. V. (2003) *Nature* **426,** 83–87
39. Qin, J., Lin, Y., Norman, R. X., Ko, H. W., and Eggenschwiler, J. T. (2011) *Proc. Natl. Acad. Sci. U.S.A.* **108,** 1456–1461
40. Huang, P., and Schier, A. F. (2009) *Development* **136,** 3089–3098
41. Lunt, S. C., Haynes, T., and Perkins, B. D. (2009) *Dev. Dyn.* **238,** 1744–1759